

- (6) Graziano, D. J.; Mackley, M. R. *Mol. Cryst. Liq. Cryst.* **1984**, *106*, 73.
- (7) Marrucci, G. *Pure Appl. Chem.* **1985**, *57*, 1545.
- (8) Wood, B. A.; Thomas, E. L. *Nature (London)* **1986**, *324*, 655.
- (9) Onogi, Y.; White, J. L.; Fellers, J. F. *J. Non-Newtonian Fluid Mech.* **1980**, *7*, 121.
- (10) Graziano, D. J.; Mackley, M. R. *Mol. Cryst. Liq. Cryst.* **1980**, *106*, 73.
- (11) Viola, G. G.; Baird, D. G. *J. Rheol.* **1986**, *30* (3), 601.
- (12) Lin, Y. G.; Winter, H. H. *Liq. Cryst.*, in press.
- (13) Lin, Y. G.; Winter, H. H.; Lieser, G. *Liq. Cryst.*, in press.
- (14) Wissbrun, K. F.; Kiss, G.; Cogswell, F. N. *Chem. Eng. Commun.* **1987**, *53*, 149.
- (15) Kiss, G. *J. Rheol.* **1986**, *30* (3), 585.
- (16) Chien, J. C. W.; Zhou, R.; Lillya, C. P. *Macromolecules* **1987**, *20*, 2340.
- (17) Dobb, M. G.; McIntyre, J. E. *J. Polym. Sci., Polym. Symp.* **1978**, *63*, 67.
- (18) Wissbrun, K. F.; Griffin, A. C. *J. Polym. Sci., Polym. Phys. Ed.* **1982**, *20*, 1835.

Pyrolysis-Field Ionization Mass Spectrometry of Epoxy Resins

Bernd Plage and Hans-Rolf Schulten*

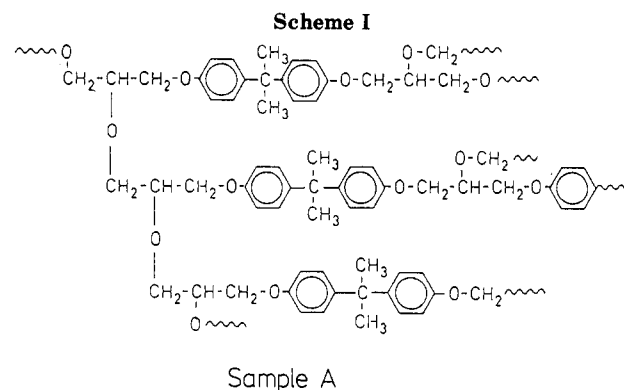
Fachhochschule Fresenius, Department of Trace Analysis, Dambachtal 20, D-6200 Wiesbaden, Federal Republic of Germany. Received October 28, 1987

ABSTRACT: The thermal degradation products formed from epoxy resins of the diglycidyl ether of bisphenol A and the tetraglycidyl ether of tetrakis(hydroxyphenyl)ethane have been investigated by temperature-resolved in-source pyrolysis-field ionization mass spectrometry (Py-FIMS). Intense signals from thermal degradation products in the mass range m/z 50–900 were detected. Molecular ions containing up to three intact bisphenol A subunits were found as main degradation products, with rearrangement reactions being involved in the formation of abundant high-mass products. Most products contain at least one phenolic end group. The temperature resolution allowed distinction between released residual monomers and dimers, and the corresponding pyrolysates formed from thermal degradation of the polymer backbone. Furthermore, epoxy resins cured with bis(aminophenyl)methane, *m*-xylenediamine, and methylhexahydrophthalic acid anhydride (MeHHPA) were investigated. Degradation products containing both bisphenol A and bis(aminophenyl)methane as well as products containing bisphenol A units and MeHHPA were observed. On the other hand, products containing amino groups were not found for the resin cured with *m*-xylenediamine.

Introduction

Mass spectrometry (MS) is a powerful tool for the investigation of technical and biological polymers.^{1–4} A wide variety of pyrolysis methods and ionization modes are now available for investigation of their thermal degradation.¹ Recently it has been demonstrated that pyrolysis (Py)-GC/MS and direct pyrolysis-field ionization (Py-FI) MS give complementary analytical results,³ and the combination of these two methods has been successfully applied to the investigation of aromatic⁵ and aliphatic⁶ polyamides. Small molecules formed by thermal degradation are identified, after separation by coupled GC, with standard electron impact (EI) MS, whereas high-mass products that are unable to pass through the capillary column are observed by FIMS. FI is a soft ionization mode that is useful for the investigation of complex mixtures, since molecular ions are predominantly formed from the thermal degradation products, with fragmentation being largely avoided.

In the present work epoxy resins prepared from the diglycidyl ether of bisphenol A (DGEBA) and from the tetraglycidyl ether of tetrakis(hydroxyphenyl)ethane (TGETE) are investigated. In addition to the corresponding pure polymers, DGEBA-based resins cured with bis(aminophenyl)methane (DDM), *m*-xylenediamine, and methylhexahydrophthalic acid anhydride (MeHHPA) are used. One sample has been prepared by curing TGETE with DDM. These samples have recently been investigated by Py-GC/MS⁷ with a pyrolysis temperature of 600 °C. In these investigations, the thermal degradation products ethylene oxide, acetaldehyde, acrolein, acetone, allyl alcohol, and phenol were observed. The DGEBA-based resins formed bisphenol A, methylated DDMs, and MeHHPA, but products containing intact *m*-xylenedi-



amine units were not observed.

The aim of our study was to monitor the presence of volatile oligomers remaining in the polymer after preparation and to investigate high-mass degradation products to obtain structural information. Indeed, products containing more than one bisphenol A unit or additional diamine units, which are not obtained by Py-GC/MS, are found in the FI spectra. The question is whether these high-mass signals can be used to give information about the linkage of the diphenol and diamine subunits.

Experimental Section

The Py-FIMS experiments were performed by using the modified⁸ direct-introduction system of a double-focusing Finnigan MAT 731 mass spectrometer. The samples were heated without any pretreatment from 50 to 750 °C in high vacuum at about 10⁻³ Pa with a heating rate of 1.2 °C s⁻¹. The mass range recorded was 50–900 daltons. The thermal degradation products were ionized at 8 kV emitter potential, and the counterelectrode was at -3 kV. All mass spectra were recorded electrically and averaged

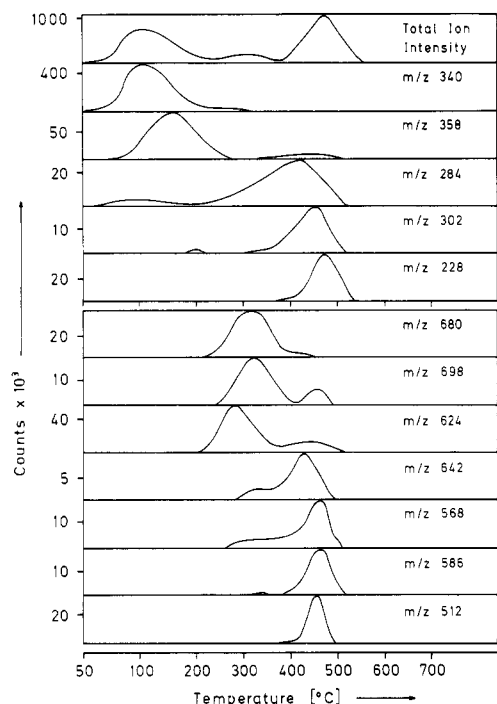


Figure 1. Sample A, temperature dependence of the formation of thermal degradation products.

with the Finnigan MAT SS 200 data system. Further experimental details have been published recently.⁸ The samples were obtained from Prof. S. Tsuge, Nagoya University, Japan, and were described in ref 7.

Results and Discussion

Sample A. Sample A was obtained by an imidazole-induced polymerization of DGEBA⁷ to give the cross-linked structure shown in Scheme I.

In the Py-FI mass spectrum the base peak at m/z 340 of sample A summed over all scans results mainly from unreacted monomer. The thermogram, i.e., the plot of the ion intensities versus the pyrolysis temperature, in Figure 1 shows the temperature dependence of the integrated ion count and the individual counts of some selected ions. The monomer at m/z 340 and in smaller amounts hydrolysis products of the monomer are released in the temperature range 50–250 °C. The hydrolysis of one of the glycidyl ether end group leads to the formation of the product observed at m/z 358 probably with a dihydroxypropyl end group. Further hydrolysis products are the monoglycidyl ether of bisphenol A (m/z 284) and dihydroxypropyl bisphenol A (m/z 302). Traces of water present in the polymer probably allow the formation of these products. The occurrence of two maxima in the thermograms indicates the different pathways for the formation of the corresponding ions. It should be noted that the ion at m/z 284 is formed in the whole temperature range from 50 to 550 °C. The first maximum at about 100 °C may be due to impurities present in DGEBA. Hydrolysis may be responsible for the formation between about 200 and 400 °C. Products appearing above about 400 °C can be assigned to pyrolysates formed by the thermal degradation of the polymer backbone. All products that are not included in Figure 1 are exclusively formed in this temperature range.

The FI signals of products containing two bisphenol A units are observed in the temperature range 250–400 °C. Tentatively assigned structures for all thermally produced chemical species mentioned in the following are included in Table I, which contains significant degradation products formed in the temperature range above 400 °C. The residual dimer appears at m/z 680, accompanied by the

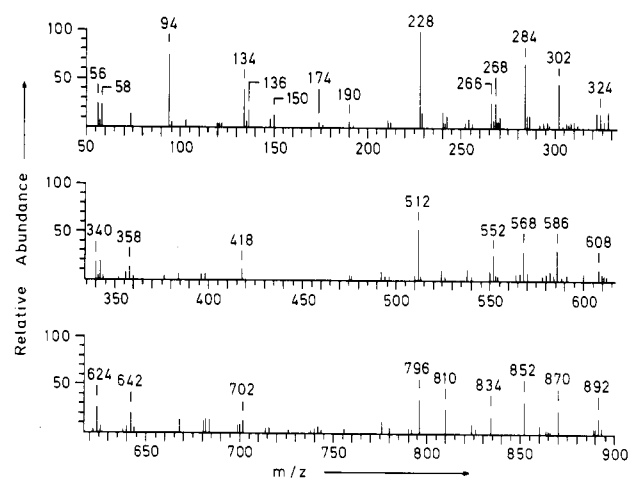


Figure 2. Sample A, summed Py-FI mass spectrum for the temperature range 400–525 °C.

partially hydrolyzed dimer at m/z 698. A possible structure of this dimer is two bisphenol A units linked by a bridging unit containing a dioxane ring (type D in Table I). The FI signal at m/z 624 can be assigned to a molecular ion, in which two units of the monoglycidyl ether of bisphenol A are linked by a hydroxypropylene group (type B in Table I). This product has already been found in the educt in amounts from 3 to 6%.⁷ The amounts can be determined from the relative abundances of the volatile components. For this, the relative abundances of products due to the monomer and those due to products containing hydroxypropylene units are summed. Provided that the sensitivities of Py-FIMS are quite similar for the components considered, the proportion of these two sums leads to a content of approximately 8%, which is in moderate agreement with the Py-GC/MS results.

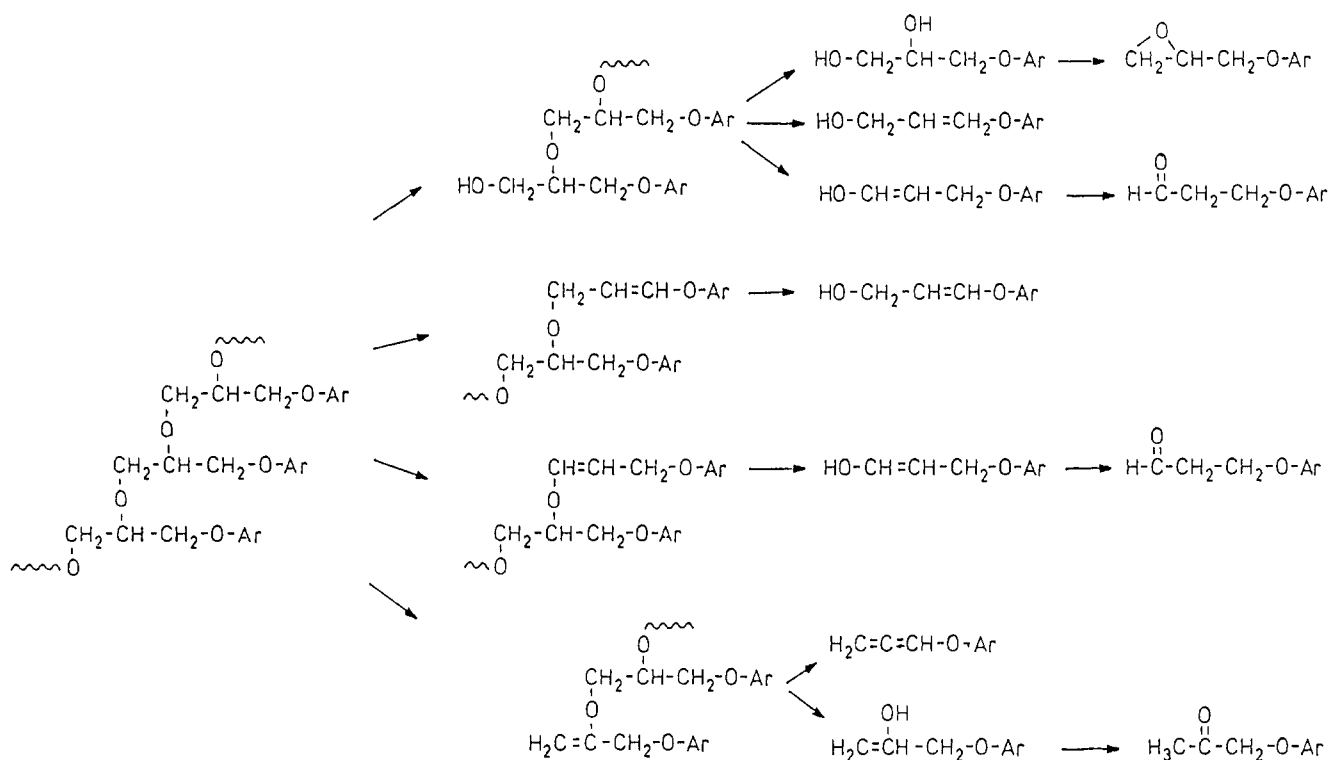
The thermal degradation of polymer A occurs mostly in the temperature range 400–525 °C. The spectrum in this range is shown in Figure 2. Structures tentatively assigned to the FI signals are given in Table I. It is probable, however, that several products with the same elemental composition are formed.

Four different structures have to be taken into account in forming the end groups R² in Tables I–V. The epoxide groups are expected to result from unreacted epoxide groups present in the polymer. As acrolein, acetone, and allyl alcohol were found by Py-GC/MS,⁷ aldehyde, methylketone, and allyl alcohol end groups are assumed to be formed under Py-FIMS conditions.

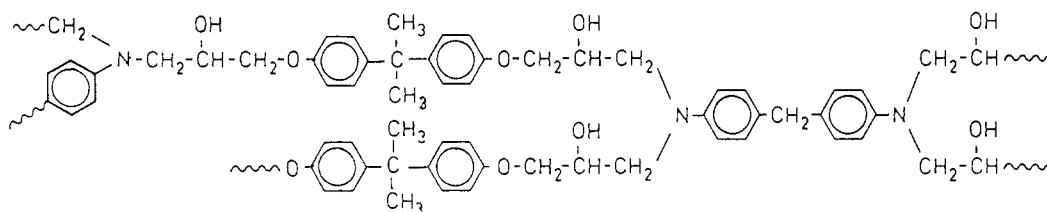
Generally, the formation of products containing phenol end groups increases with increasing temperature. Simultaneously, the formation of products containing epoxide, methylketo, or aldehyde end groups decreases. Evidently, the structure of products appearing above m/z 512 with high abundance is not in agreement with the original polymer structure. The dominant mass signals at m/z 512 and 796 are assigned to a diphenol in which the bisphenol A subunits are linked by hydroxypropylene. The high amounts of these degradation products exclude that they are formed only by scissions of bonds of the polymer backbone. Only the impurities in the educt (3–8%) contain substructures found in these degradation products. Thus, ether-exchange reactions must occur prior to thermal fragmentation. Aliphatic ether groups are replaced by aliphatic–aromatic ether bonds leading to groups of two phenyleneoxy groups linked by hydroxypropylene.

Many CH-transfer reactions, rearrangements, and exchange reactions have been observed for linear polyethers, including polymers containing bisphenol A and aliphatic

Scheme II



Scheme III



Sample B

subunits.^{9,10} If the aliphatic moieties consisted of at least two methylene groups, β -CH-transfer reactions were found as main degradation pathways leading to olefinic bonds and hydroxy end groups. The same mechanisms may operate for cross-linked polymers such as epoxy resins in the formation of the hydroxy, aldehyde, and keto functions in the degradation products of sample A as shown in Scheme II. On the other hand, the phenolic end groups may also be formed by a β -CH-transfer reaction. More complex mechanisms for the formation of methylcarbonyl and propenyl end groups have been described.¹¹

In Py-FIMS, exchange reactions are involved in the formation of bisphenol A units linked by hydroxypropylene groups. These structures are present only in very low amounts in the original polymer and, thus, result mainly from ether-exchange reactions. These have already been described for linear aromatic-aliphatic polyethers.¹⁰ Probably, the formation of such structures yields the most stable products formed in an equilibrium of ether-exchange reactions.

Some FI signals are assigned to products of type B as well as type D (Table I). These products appear in a broad temperature range from 250 to 500 °C. It can be assumed that products containing the substructure D are predominantly formed below 400 °C (hydrolysis products of free dimer), whereas products containing structure B are mainly formed above 400 °C with the onset of the rearrangement reactions (degradation of the polymer back-

bone). The two different origins of products observed at the same m/z value is indicated in the thermograms by the appearance of two maxima or a broad shoulder.

The formation of phenol, isopropylphenol, and isopropenylphenol increases with increasing temperature. In addition, products terminated by a isopropenyl end group are observed, for example, at m/z 190, 418, and 702. In general, these ions appear 94 mass units below high abundant signals assigned to a phenol or diphenol listed in Table I. The second possibility for cleavage of bisphenol A units leads to products terminated by phenyl groups indicated by signals 134 mass units below the corresponding signals related to phenols. These are less abundant than those assigned to products terminated by isopropenylphenyl end groups. Similar effects are seen in the Py low-energy EI mass spectra of linear aliphatic-aromatic polyethers containing bisphenol A units.¹⁰

Mass signals observed 14 mass units higher than the diphenols are seen at m/z 242, 524, and 810 and can be assigned to methyl ethers. Methyl ethers of phenol, isopropylphenol, and isopropenylphenol appear at m/z 108, 148, and 150. A further possible end group is hydroxypropyl. Products containing this end group are indicated by signals appearing two mass units higher than those of the corresponding glycidyl ethers. Such ions are observed at m/z 286, 326, 342, 570, 610, 626, 644, 682, and 700. Signals assigned to bis(hydroxypropyl) compounds are seen at m/z 344 and 684. Products terminated by an allyl end

Table I
Structures Assigned to Thermal Degradation Products of Sample A

Structure	m/z (Rel. abundance %)	
$R^1 - \underline{A}$	R^1	228 (100)
	R^2	284 (67)
	R^3	302 (47)
	R^4	268 (28)
$R^2 - \underline{A}$	R^2	340 (17)
	R^3	358 (14)
	R^4	324 (12)
$R^3 - \underline{A}$	R^3	376 (5)
	R^4	342 (22)
$R^4 - \underline{A}$	R^4	308 (7)
$R^1 - \underline{B}$	R^1	512 (52)
	R^2	568 (29)
	R^3	586 (31)
	R^4	552 (26)
$R^2 - \underline{B}$ or $R^1 - \underline{D}$	R^2	624 (28)
	R^3	642 (17)
	R^4	608 (11)
$R^3 - \underline{B}$	R^3	660 (4)
	R^4	626 (8)
$R^4 - \underline{B}$	R^4	592 (6)
$R^2 - \underline{D}$	R^2	680 (3)
	R^3	698 (7)
	R^4	664 (6)
$R^3 - \underline{D}$	R^3	716 (4)
	R^4	682 (9)
$R^4 - \underline{D}$	R^4	648 (2)
$R^1 - \underline{C}$	R^1	796 (35)
	R^2	852 (29)
	R^3	870 (26)
	R^4	836 (3)
$R^2 - \underline{C}$	R^4	892 (15)

$$R-O-\text{C}_6\text{H}_4-\text{C}(\text{CH}_3)_2-\text{C}_6\text{H}_4-O-[CH_2-\underset{\text{OH}}{\text{CH}}-CH_2-O-\text{C}_6\text{H}_4-\text{C}(\text{CH}_3)_2-\text{C}_6\text{H}_4-O]_x-R$$

$\underline{A}; \underline{B}; \underline{C} \quad x = 0; 1; 2$

$$R-O-\text{C}_6\text{H}_4-\text{C}(\text{CH}_3)_2-\text{C}_6\text{H}_4-O-CH_2-\underset{\text{O}}{\text{CH}}-\underset{\text{O}}{\text{CH}}-CH_2-O-\text{C}_6\text{H}_4-\text{C}(\text{CH}_3)_2-\text{C}_6\text{H}_4-O-R$$

\underline{D}

$R^1 = \sim H$

$R^2 = \sim CH_2-\underset{\text{O}}{\text{CH}}-CH_2 \ ; \ \sim CH=CH-CH_2OH \ ;$

$\sim CH_2-\underset{\text{O}}{\text{C}}-CH_3 \ ; \ \sim CH_2-CH_2-CHO$

$R^3 = \sim CH_2-\underset{\text{OH}}{\text{CH}}-CH_2OH$

$R^4 = \sim CH_2-CH=CH_2$

group are observed at m/z 266, 322, 550, and 834.

Sample B. Sample B was prepared by the polymerization of DGEBA with 25 wt % DDM.⁷ The primary amine reacts with two epoxy groups, forming a tertiary amine and two secondary alcoholic groups (see Scheme III).

In Py-FIMS, the total ion current shows a sharp maximum at 430 °C; no volatiles resulting from unreacted educts are observed at lower temperatures. The summed FI mass spectrum is shown in Figure 3, and the products assigned to the signals are listed in Table II. Generally, bisphenol as well as diamine subunits are found in the degradation products. As observed by Py-GC/MS,⁷ methylated amines are preferred to unsubstituted amines. Only traces of DDM are recovered, but large amounts of tetramethyl DDM are formed. The relative abundances of signals corresponding to methylated amines increase with increasing numbers of methyl substituents at the amino groups. Degradation products containing bisphenol A units are mainly terminated by phenol or aldehyde end groups.

Several products contain one bisphenol A unit and one DDM unit linked by a hydroxypropylene group. Different structures are involved in the formation of some signals, as shown in Table II. As such products, which contain *N*-methyl groups, are preferred to unsubstituted amines, the abundances of the ions at m/z 566 and 580 indicate

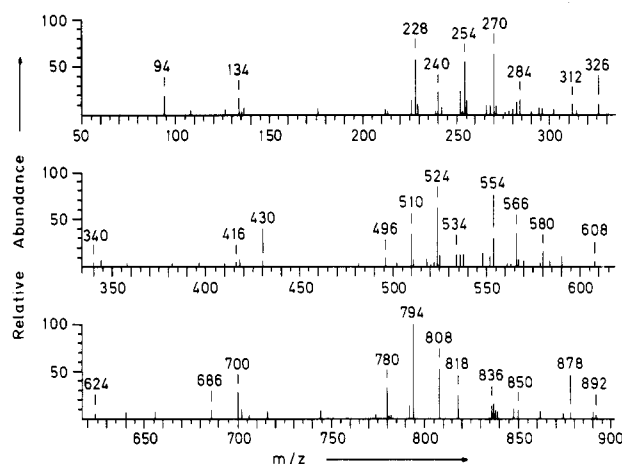


Figure 3. Sample B, summed Py-FI mass spectrum for the temperature range 50–750 °C.

that the former is produced mainly by the aldehyde-terminated product containing three *N*-methyl bonds. By analogy, the product at m/z 524 is mainly assigned to the phenol derivative containing three *N*-methyl groups. The signals at m/z 534 and 548 are due to the loss of water from the products observed at m/z 552 and 566 and are also listed in Table II.

Table II
Structures Assigned to Thermal Degradation Products of Sample B

m/z (Rel. abundance %)		
198 (2), 212 (5), 226 (15), 240 (24), 254 (56)		
R = H/CH ₃		

$$R_2N-\text{C}_6\text{H}_4-\text{CH}_2-\text{C}_6\text{H}_4-\text{NR}_2$$

R	R	
R ¹	R ¹	228 (58)
	R ²	284 (17)
	R ³	302 (8)
	R ⁴	268 (11)
	R ⁵	270 (63)
R ²	R ²	340 (4)
	R ³	358 (3)
	R ⁴	324 (2)
	R ⁵	326 (12)
R ³	R ⁵	344 (7)
R ⁵	R ⁵	312 (12)

$$R-O-\text{C}_6\text{H}_4-\text{C}(\text{CH}_3)_2-\text{C}_6\text{H}_4-O-R$$

$R^1 = \sim H$
 $R^2 = \sim CH_2-\text{CH}(\text{O})-\text{CH}_2$; $\sim CH=CH-\text{CH}_2\text{OH}$;
 $\sim CH_2-\overset{\text{O}}{\underset{\text{O}}{\text{C}}}-\text{CH}_3$; $\sim CH_2-\text{CH}_2-\text{CHO}$
 $R^3 = \sim CH_2-\overset{\text{OH}}{\underset{\text{O}}{\text{C}}}-\text{CH}_2\text{OH}$
 $R^5 = \sim CH_2-\text{CHO}$

R	R'	
R ¹	H H H	482 (3)
	H H CH ₃	496 (10)
	H CH ₃ CH ₃	510 (36)
R ¹	CH ₃ CH ₃ CH ₃	524 (63)
	H H H	524 (63)
R ²	H H H	538 (14)
	H H CH ₃	538 (14)
R ²	H H CH ₃	552 (15)
	H CH ₃ CH ₃	552 (15)
R ²	H CH ₃ CH ₃	566 (36)
	CH ₃ CH ₃ CH ₃	566 (36)
R ²	CH ₃ CH ₃ CH ₃	580 (18)

$$R-O-\text{C}_6\text{H}_4-\text{C}(\text{CH}_3)_2-\text{C}_6\text{H}_4-O-\text{CH}_2-\overset{\text{OH}}{\underset{\text{O}}{\text{C}}}-\text{CH}_2-\text{N}(\text{R}')-\text{C}_6\text{H}_4-\text{CH}_2-\text{C}_6\text{H}_4-\text{NR}'_2$$

R	R	
R ¹	R ¹	794 (100)
	R ²	850 (6)
	R ³	868 (5)
	R ⁵	836 (14)
R ²	R ⁵	892 (4)
R ⁵	R ⁵	873 (7)

$$R-O-\text{C}_6\text{H}_4-\text{C}(\text{CH}_3)_2-\text{C}_6\text{H}_4-O-\text{CH}_2-\overset{\text{OH}}{\underset{\text{O}}{\text{C}}}-\text{CH}_2-\text{N}(\text{R}')-\text{C}_6\text{H}_4-\text{CH}_2-\text{C}_6\text{H}_4-\text{N}(\text{R}')-\text{CH}_2-\overset{\text{OH}}{\underset{\text{O}}{\text{C}}}-\text{CH}_2-O-\text{C}_6\text{H}_4-\text{C}(\text{CH}_3)_2-\text{C}_6\text{H}_4-O-R$$

R	
R ¹	808 (64)
R ²	864 (7)
R ³	832 (1)
R ⁴	848 (10)
R ⁵	850 (10)

$$R-\left[O-\text{C}_6\text{H}_4-\text{C}(\text{CH}_3)_2-\text{C}_6\text{H}_4-O-\text{CH}_2-\overset{\text{OH}}{\underset{\text{O}}{\text{C}}}-\text{CH}_2\right]_2-\text{N}(\text{CH}_3)-\text{C}_6\text{H}_4-\text{CH}_2-\text{C}_6\text{H}_4-\text{N}(\text{CH}_3)_2$$

x	
0	270 (63)
1	554 (32)
2	838 (8)

$$R-O-\left[\text{C}_6\text{H}_4-\text{C}(\text{CH}_3)_2-\text{C}_6\text{H}_4-O-\text{CH}_2-\overset{\text{OH}}{\underset{\text{O}}{\text{C}}}-\text{CH}_2\right]_x-\text{C}_6\text{H}_4-\text{C}(\text{CH}_3)_2-\text{C}_6\text{H}_4-O-\text{CH}_2-\text{CHO}$$

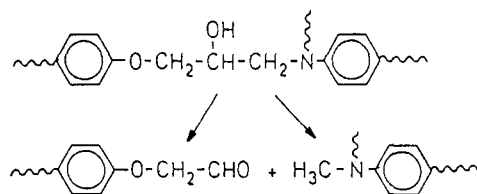
Phenols and N-H bonds may result from β -CH-transfer reactions. The preferred mechanism observed is the formation of degradation products terminated by aldehyde and N-methyl groups as shown in Scheme IV.

Abundant high-mass signals are observed for products containing two bisphenol A and one DDM units. The corresponding molecular ion of the diphenol forms the base peak at m/z 794. The signal at m/z 808 may be assigned to the methyl ether or an alternative structure listed in

Table II. Signals of degradation products containing N-H bonds are only seen in association with very high abundant signals related to fully substituted amines, for example, at m/z 780.

A series of abundant signals is found at m/z 270, 554, and 838, assigned to pyrolyzates terminated with one phenolic and one aldehyde end group. The members of this series differ in the number of additional bisphenol A units linked by hydroxypropylene groups. Surprisingly,

Scheme IV



no abundant signals of the corresponding diphenols (m/z 512 and 796) or dialdehydes (m/z 596 and 880) are observed. The reason for the absence of these signals is not clear. On the other hand, the relative abundance of the dialdehyde at m/z 312 is low, whereas the abundance of the monoaldehyde at m/z 270 is very high. A further series differing in one bisphenol A and one hydroxypropylene unit is seen at m/z 534 and 818. The ion at m/z 534 is expected to be a phenol accompanied by the corresponding glycidyl ether at m/z 590.

In addition to ether-exchange reactions, exchange reactions between amine and ether can be expected. As with the formation of bisphenol A units linked by hydroxypropylene, two trimethyl-DDM units bound by hydroxypropylene may result in the formation of the ion at m/z 536 (23% relative abundance). A subsequent CH-transfer reaction leads to the formation of products in which methyl and acetaldehyde groups appear as substituents at the nitrogen. These aldehydes are observed 28 mass units above the abundant signals assigned to dimethylamines and are seen, for example, at m/z 282, 552, 608, 836, and 878.

As with sample A, the cleavage of the bisphenol unit can occur to give products 94 mass units below high abundant mass signals assigned to phenols. Such ions are observed at m/z 176, 416, 430, 686, and 700. Phenol as well as isopropyl- and isopropenylphenol is detected in high abundance.

The absence of abundant odd number mass signals indicates that the formation of products resulting from the fission of a DDM unit is excluded.

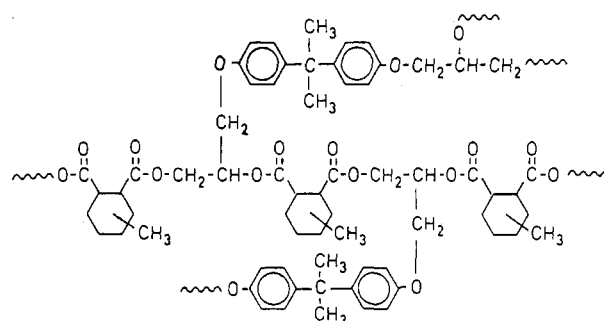
Sample C. Sample C was prepared from DGEBA and 17 wt % *m*-xylenediamine.⁷ The structure is expected to be similar to that shown for sample B.

Only small amounts of DGEBA are observed at low temperatures; products related to the diamine are not seen. The averaged spectrum for the whole temperature range shows many low abundant signals up to m/z 900 and only a few of moderate abundance. As with sample B, bisphenol units with the end groups phenol, epoxide, and aldehyde are observed at m/z 228, 340, and 270. Further, signals already described for samples A and B in Tables I and II appear at m/z 284, 302, 326, 340, and 244. Phenol is not found, but isopropenylphenol is seen at m/z 134 with 9% relative abundance. Abundant signals are observed at m/z 418 (88%) and m/z 512 (23%). It is possible that the ion at m/z 512 is due to the same diphenol as in sample A. Splitting of the bisphenol A unit is involved in the formation of the ion at m/z 418. In addition, for both products the molecular ions of the corresponding aldehydes are detected at m/z 460 (11%) and 554 (12%).

Obviously, the structure of the diamine unit is important for the degradation pathway. However, steric effects have to be taken into account. Although aldehydes are formed also in sample B, the corresponding *N*-methyl products are not observed. It seems that these products undergo further reactions to give the low abundant high-mass signals.

Sample D. Sample D was prepared from DGEBA and 80 wt % MeHHPA.⁷ In addition to ether bonds, this

Scheme V



Sample D

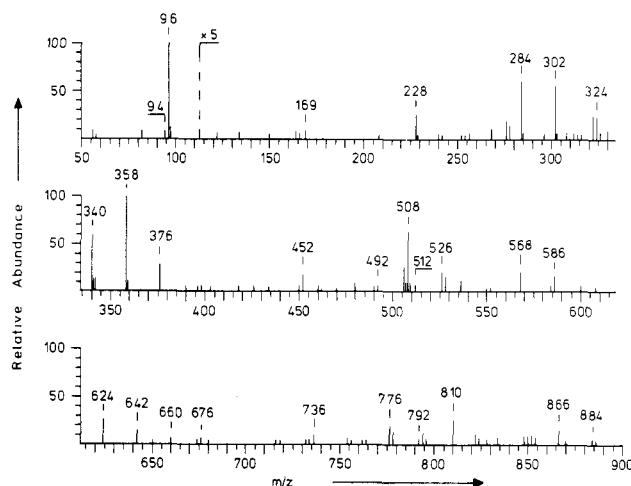


Figure 4. Sample D, summed Py-FI mass spectrum for the temperature range 50–750 °C.

polymer contains large amounts of ester bonds and has to be considered as a mixed polyether/polyester compound (Scheme V).

The sample contains volatile DGEBA, and, in smaller amounts, the related hydrolysis products are seen at m/z 284 and 358. Moreover, volatiles are found at m/z 67, 94, 96, 122, and 166, which may be assigned to residual solvents, phenol or methylcyclohexadiene, methylcyclohexene, benzoic acid, and tetrahydrophthalic acid, which are probably impurities in MeHHPA. In contrast to results from Py-GC/MS, only traces of MeHHPA are recovered under Py-FIMS conditions, indicating different thermal degradation pathways for flash Py and Py-MS using the direct introduction system.

The Py-FI mass spectrum of sample D is shown in Figure 4. Table III assigns the main signals observed to the corresponding thermal degradation products. The main degradation product forming the base peak at m/z 96 is the molecular ion of methylcyclohexene, which represents about 23% of the total ion intensity. High abundant signals due to products containing dihydropropyl end groups are seen, whereas products containing aldehyde end groups are absent. Several products found in sample A are observed for sample D. The formation of phenyl end groups is much lower than in samples A, B, and C.

In contrast to sample A, the abundances of products terminated by dihydroxypropyl end groups is much higher. In addition, many products are probably terminated by ketene end groups. The formation of ketene and hydroxy end groups from polyesters has been observed by using electron impact (EI) mass spectrometry¹² but was not observed with chemical ionization (CI).¹³ With Py-FIMS, signals due to ketenes or alcohols are also missing.¹⁴ On

Table III
Structures Assigned to Thermal Degradation Products of Sample D

m/z (Rel. abundance %)	R	R	
R ¹ R ¹	228 (5)		R ¹ = ~H
R ¹ R ²	284 (12)		R ² = ~CH ₂ -CH(O)-CH ₂ ; ~CH=CH-CH ₂ OH
R ¹ R ³	302 (11)		~CH ₂ -C(=O)-CH ₃ ; ~CH ₂ -CH ₂ -CHO
R ¹ R ⁴	268 (2)		R ³ = ~CH ₂ -CH(OH)-CH ₂ OH
R ² R ²	340 (12)		R ⁴ = ~CH ₂ -CH=CH ₂
R ² R ³	358 (20)		
R ² R ⁴	324 (4)		
R ³ R ³	376 (6)		
R ³ R ⁴	342 (3)		
R ⁴ R ⁴	308 (1)		
R ¹ R ¹	512 (2)		
R ¹ R ²	568 (4)		
R ¹ R ³	586 (3)		
R ² R ²	624 (5)		
R ² R ³	642 (3)		
R ³ R ³	660 (1)		
R ¹ R ²	452 (4)		
R ² R ²	508 (13)		
R ³ R ³	526 (5)		
R ⁴ R ⁴	492 (2)		
R ¹ R ²	736 (2)		
R ² R ²	792 (1)		
R ³ R ³	810 (5)		
R ⁴ R ⁴	776 (4)		
	676 (1)		
R ¹ R ¹	754 (1)		
R ¹ R ²	810 (5)		
R ¹ R ³	828 (1)		
R ² R ²	866 (3)		
R ² R ³	884 (1)		

one hand, fragmentation like with EI does not take place with polyesters under the experimental conditions employed; on the other hand, ketenes are observed for sample D although ketenes are absent in CI or FI spectra of polyesters. Predominantly cyclic oligomers have been found.¹³ The cross-linked structure of sample D may be responsible for the different behavior. In contrast to linear polyesters, the formation of cyclic structures from cross-linked networks is difficult. Thus, alternative degradation pathways may occur. A further possible way is a β -CH transfer, forming olefin and carboxylic acid.^{9,13} This reaction involves a six-membered transition state and can be expected to be unfavorable for fixed structures. To a lesser extent this reaction takes place. For sample D, after acid formation a subsequent intramolecular condensation reaction forms MeHHPA.

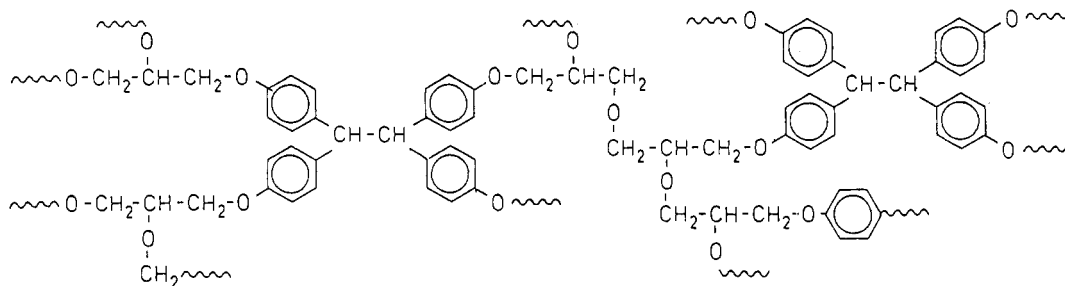
As well-known degradation pathways are unfavorable, a CH-transfer reaction forming ketene and alcohol can be assumed. In comparison with sample A, the much higher abundances for products terminated with dihydroxypropyl end groups indicate that the hydrogen necessary for alcohol formation results from the ester subunits.

The formation of methylcyclohexene may result from fission between the carbonyl group and the cyclohexene ring followed by splitting of the second carbonyl group. Elimination of the remaining carbonyloxy group leads to glycidyl ether end groups and decarbonylation to dihydroxypropyl end groups.

Sample E. Sample E was prepared from TGETE.⁷ This polymer differs from sample A in the structure of the aromatic subunits, whereas the linkages between these units are the same as those present in sample A (Scheme VI).

Several pyrolysis products below 400 °C are observed at m/z 126, 196, 256, 266, 284, 311, 312, 428, 438, and 588. No molecular ion of TGETE is seen at m/z 622. At about 300 °C the base peak at m/z 311 results from volatile monomer which has been split thermally into two equal radicals. The aliphatic carbon-carbon bond is expected to be the weakest bond in a polymer based on TGETE. The formation of doubly charged molecular ions of TGETE, which would also appear at m/z 311, can be excluded because no corresponding isotopic peak can be seen at m/z 311.5. As TGETE itself is unstable even at

Scheme VI



Sample E

Table IV
Structures Assigned to Thermal Degradation Products of Samples E

m/z (Rel. abundance)*

Skeleton

R	R	<u>E</u>	<u>F</u>	<u>G</u>
	R ¹	200 (6/100)	210 (11/45)	316 (2/50)
R ¹	R ²	256 (41/46)	266 (42/12)	372 (9/14)
	R ³	274 (4/28)	284 (-/8)	390 (2/13)
R ²	R ²	312 (100/12)	322 (2/1)	428 (31/4)
	R ³	330 (14/20)	340 (1/13)	446 (3/9)
R ³	R ³	348 (1/3)	358 (3/9)	464 (1/1)

Number of
skeletons

m/z (Rel. abundance)**

<u>E</u>	<u>F</u>	<u>G</u>	R=R ¹ /R ¹	R=R ¹ /R ²	R=R ¹ /R ³
2	0	0	456 (22)	512 (8)	530 (7)
0	2	0	476 (3)	532 (2)	550 (5)
0	0	2	688 (9)	744 (5)	762 (-)
1	1	0	466 (9)	522 (11)	540 (5)
1	0	1	572 (25)	628 (13)	640 (10)
0	1	1	582 (23)	638 (11)	656 (11)
3	0	0	712 (17)	768 (6)	786 (2)
2	1	0	722 (6)	778 (-)	796 (-)
2	0	1	828 (6)	884 (-)	
1	1	1	838 (6)	894 (-)	

E

$$\text{R-O}-\text{C}_6\text{H}_4-\text{CH}_2-\text{C}_6\text{H}_4-\text{O-R}$$

F

$$\text{R-O}-\text{C}_6\text{H}_4-\text{C}\equiv\text{C}-\text{C}_6\text{H}_4-\text{O-R}$$

G

R-O-unknown structure-O-R

R¹ = ~H

R² = ~CH₂-CH(O)-CH₂ ; ~CH=CH-CH₂OH ;

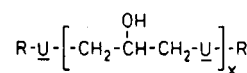
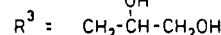
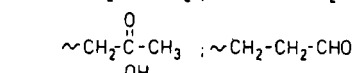
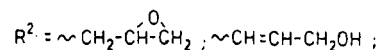
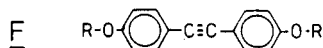
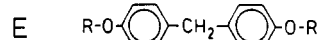
$$\sim\text{CH}_2-\overset{\text{O}}{\underset{\text{||}}{\text{C}}}-\text{CH}_3 ; \sim\text{CH}_2-\text{CH}_2-\text{CHO}$$

R³ = ~CH₂-CH(OH)-CH₂OH

$$\text{R}-\underline{\text{U}}-\left[-\text{CH}_2-\overset{\text{OH}}{\underset{|}{\text{CH}}}-\text{CH}_2-\underline{\text{U}}\right]_x-\text{R}$$

x = 0;1;2

U = unit E, F, or G



* relative abundances in the temperature ranges 350 to 400 °C and 400 to 600 °C

** relative abundance for the summed spectrum over the whole temperature range

300 °C, no other thermal degradation products containing intact TGETE units can be observed at higher temperatures.

With increasing temperature the abundance of the ion at m/z 311 decreases and, at the same time, the formation of m/z 312 increases. This can be explained by an inter- or intramolecular hydrogen-transfer reaction of the radical formed first with the polymer backbone.

The summed FI spectrum of the whole temperature range is shown in Figure 5. As observed for sample A, products containing the same aromatic unit appear in the order diglycidyl ether, monoglycidyl ether, and diphenol with rising temperature. Subunits involved in these series are bis(hydroxyphenyl)methane, forming ions at m/z 312, 256, and 200 and bis(hydroxyphenyl)acetylene, forming ions at m/z 266 and 210. A high abundant signal appears at m/z 316. Since there is a difference of 56 mass units between the phenols and epoxides, the appearance of the ions at m/z 372 and 428 leads to the assumption that the species seen at m/z 316 can be assigned to a diphenol.

The summed mass spectrum for the temperature range above 400 °C shows mass signals of mostly even nominal masses in the mass range from 300 to 700 daltons with

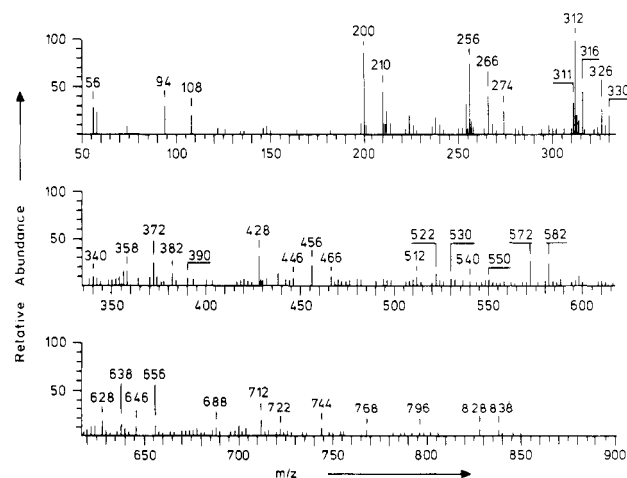
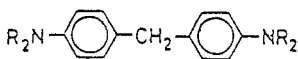
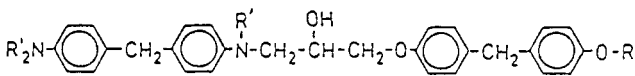
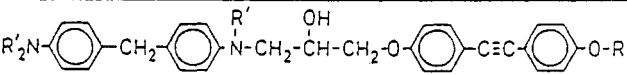
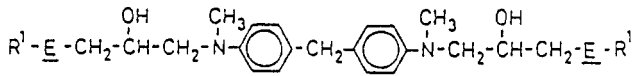
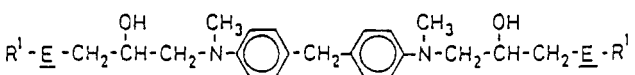


Figure 5. Sample E, summed Py-FI mass spectrum for the temperature range 50-750 °C.

about 5% relative abundance. Therefore, only high abundant mass signals are useful for interpretation. Structures assigned to these significant mass signals are

Table V
Structures Assigned to Thermal Degradation Products of Sample F

<p>m/z (Rel. abundance %)</p> <p>198 (21), 212 (26), 226 (52), 240 (56), 254 (30)</p> <p>$R' = H/CH_3$</p>																																									
<table> <tr> <th>R</th><th>R</th><th>E</th><th>F</th><th>G</th></tr> <tr> <td>R^1</td><td></td><td>200 (100)</td><td>210 (27)</td><td>316 (58)</td></tr> <tr> <td>$R^1 R^2$</td><td></td><td>256 (27)</td><td>266 (23)</td><td>372 (11)</td></tr> <tr> <td>R^3</td><td></td><td>274 (13)</td><td>284 (4)</td><td>390 (6)</td></tr> <tr> <td>R^5</td><td></td><td>242 (41)</td><td>252 (39)</td><td>358 (23)</td></tr> <tr> <td>$R^2 R^2$</td><td></td><td>312 (12)</td><td>322 (1)</td><td>428 (3)</td></tr> </table>	R	R	E	F	G	R^1		200 (100)	210 (27)	316 (58)	$R^1 R^2$		256 (27)	266 (23)	372 (11)	R^3		274 (13)	284 (4)	390 (6)	R^5		242 (41)	252 (39)	358 (23)	$R^2 R^2$		312 (12)	322 (1)	428 (3)	<p>E $R-O-\text{C}_6\text{H}_4-\text{CH}_2-\text{C}_6\text{H}_4-O-R$ $R^1 = \sim H$</p> <p>F $R-O-\text{C}_6\text{H}_4-C\equiv C-\text{C}_6\text{H}_4-O-R$ $R^2 = \sim CH_2-\overset{O}{\underset{O}{\text{C}}}-CH_2 \sim ; \sim CH=CH-CH_2OH ;$ $\sim CH_2-\overset{O}{\underset{OH}{\text{C}}}-CH_3 \sim ; \sim CH_2-CH_2-CHO$</p> <p>G $R-O$-unknown structure-$O-R$ $R^3 = \sim CH_2-\overset{OH}{\text{C}}-CH_2OH$</p>										
R	R	E	F	G																																					
R^1		200 (100)	210 (27)	316 (58)																																					
$R^1 R^2$		256 (27)	266 (23)	372 (11)																																					
R^3		274 (13)	284 (4)	390 (6)																																					
R^5		242 (41)	252 (39)	358 (23)																																					
$R^2 R^2$		312 (12)	322 (1)	428 (3)																																					
<table> <tr> <th>R</th><th>R</th><th>R'</th></tr> <tr> <td>R^1</td><td>H</td><td>H</td></tr> <tr> <td>R^1</td><td>H</td><td>CH₃</td></tr> <tr> <td>R^5</td><td>H</td><td>CH₃</td></tr> <tr> <td>R^1</td><td>CH₃</td><td>CH₃</td></tr> <tr> <td>R^5</td><td>H</td><td>H</td></tr> <tr> <td>R^5</td><td>H</td><td>CH₃</td></tr> <tr> <td>R^5</td><td>H</td><td>CH₃</td></tr> <tr> <td>R^5</td><td>CH₃</td><td>CH₃</td></tr> <tr> <td>R^2</td><td>CH₃</td><td>CH₃</td></tr> </table>	R	R	R'	R^1	H	H	R^1	H	CH ₃	R^5	H	CH ₃	R^1	CH ₃	CH ₃	R^5	H	H	R^5	H	CH ₃	R^5	H	CH ₃	R^5	CH ₃	CH ₃	R^2	CH ₃	CH ₃											
R	R	R'																																							
R^1	H	H																																							
R^1	H	CH ₃																																							
R^5	H	CH ₃																																							
R^1	CH ₃	CH ₃																																							
R^5	H	H																																							
R^5	H	CH ₃																																							
R^5	H	CH ₃																																							
R^5	CH ₃	CH ₃																																							
R^2	CH ₃	CH ₃																																							
<table> <tr> <td>R^1</td><td>CH₃</td><td>CH₃</td><td>CH₃</td><td>506 (11)</td></tr> <tr> <td>R^5</td><td>CH₃</td><td>CH₃</td><td>CH₃</td><td>568 (9)</td></tr> <tr> <td>R^1</td><td>H</td><td>H</td><td>H</td><td>570 (6)</td></tr> <tr> <td>R^1</td><td>H</td><td>H</td><td>CH₃</td><td>584 (10)</td></tr> <tr> <td>R^1</td><td>H</td><td>CH₃</td><td>CH₃</td><td>598 (22)</td></tr> <tr> <td>R^1</td><td>CH₃</td><td>CH₃</td><td>CH₃</td><td>612 (29)</td></tr> <tr> <td>R^5</td><td>H</td><td>CH₃</td><td>CH₃</td><td>640 (7)</td></tr> <tr> <td>R^5</td><td>CH₃</td><td>CH₃</td><td>CH₃</td><td>654 (9)</td></tr> </table>	R^1	CH ₃	CH ₃	CH ₃	506 (11)	R^5	CH ₃	CH ₃	CH ₃	568 (9)	R^1	H	H	H	570 (6)	R^1	H	H	CH ₃	584 (10)	R^1	H	CH ₃	CH ₃	598 (22)	R^1	CH ₃	CH ₃	CH ₃	612 (29)	R^5	H	CH ₃	CH ₃	640 (7)	R^5	CH ₃	CH ₃	CH ₃	654 (9)	
R^1	CH ₃	CH ₃	CH ₃	506 (11)																																					
R^5	CH ₃	CH ₃	CH ₃	568 (9)																																					
R^1	H	H	H	570 (6)																																					
R^1	H	H	CH ₃	584 (10)																																					
R^1	H	CH ₃	CH ₃	598 (22)																																					
R^1	CH ₃	CH ₃	CH ₃	612 (29)																																					
R^5	H	CH ₃	CH ₃	640 (7)																																					
R^5	CH ₃	CH ₃	CH ₃	654 (9)																																					
<table> <tr> <td></td><td>456 (8)</td></tr> <tr> <td></td><td>466 (6)</td></tr> <tr> <td></td><td>572 (14)</td></tr> <tr> <td></td><td>582 (10)</td></tr> <tr> <td></td><td>638 (3)</td></tr> </table>		456 (8)		466 (6)		572 (14)		582 (10)		638 (3)	$R^1-E-H-E-R^1$ $R^1-E-H-F-R^1$ $R^1-E-H-G-R^1$ $R^1-F-H-G-R^1$ $R^1-G-H-G-R^1$ $H = \sim CH_2-\overset{OH}{\text{C}}-CH_2 \sim$																														
	456 (8)																																								
	466 (6)																																								
	572 (14)																																								
	582 (10)																																								
	638 (3)																																								
<table> <tr> <td></td><td>738 (11)</td></tr> </table>		738 (11)																																							
	738 (11)																																								
<table> <tr> <td></td><td>748 (4)</td></tr> </table>		748 (4)																																							
	748 (4)																																								

listed in Table IV. Three types of subunits, E, F, and G, are involved in the formation of these high-mass signals. Bis(hydroxyphenyl)methane, bis(hydroxyphenyl)acetylene, and the chemical species observed at m/z 316 are linked by hydroxypropylene units. The relative abundances are given for the temperature ranges up to 400 °C and above 400 °C, indicating the preference of glycidyl ethers at lower temperatures and the formation of the m/z 316 subunit at higher temperatures.

In particular, products containing phenolic end groups are observed. Products containing one glycidyl ether end group are detected at the beginning of the formation of the corresponding diphenol.

As with sample A, exchange reactions are involved in the formation of hydroxypropylene units bridging the

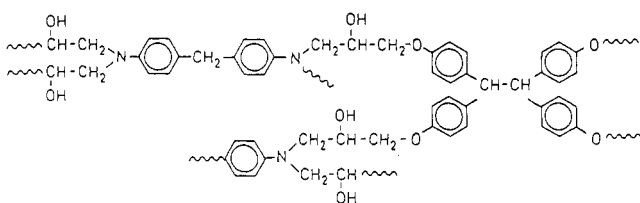
aromatic subunits. Because of the weak carbon-carbon bond of tetraphenylethane, radicals are formed that might be responsible for the formation of a large number of different products observed in the upper mass range with low relative abundance.

As seen from the other samples, the formation of phenols indicated by the ion at m/z 94 increases with rising temperature. At present, no reason can be given for the abundant product at m/z 700.

Sample F. Sample F was prepared from TGETE and 25 wt % DDM.⁷ The aromatic subunits in the polymer are identical with those in sample E, and the linkages between the epoxide and amine subunits are the same as in sample B (Scheme VII).

The main thermal degradation products are terminated

Scheme VII



Sample F

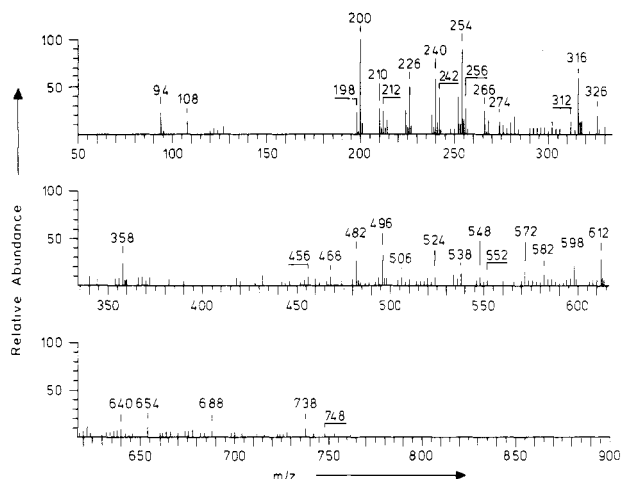


Figure 6. Sample F, summed Py-FI mass spectrum for the temperature range 50–750 °C.

by phenols and, with lower abundances, by aldehyde end groups. As with sample B, which also contains DDM, degradation products containing methylated DDM subunits are found. The relative abundance of glycidyl ethers is very low, and volatiles are not observed.

The FI spectrum is given in Figure 6. As with sample E, many mass signals with about 5% relative abundance are seen. Structures assigned to more abundant thermal degradation products are listed in Table V. Many products containing one DDM unit linked by the subunits described for sample E are observed. Probably not all TGETE units are bound to DDM. High-mass signals common to sample E are observed at m/z 456, 466, 572, 582, and 688, indicating areas in the polymer that are free of DDM. These regions are identical with the structure of sample E. In contrast, sample B forms only very low amounts of high-mass products free of DDM.

As with sample E, no intact tetraphenylethane units are observed in the degradation products. For the formation of aldehyde and *N*-methyl end groups the same mechanism as shown for sample B is involved.

Conclusions

The majority of the high-mass signals of the thermal degradation products are not due to the original polymer structure of the DGEBA polymers. Intramolecular ether-ether exchange reactions can be expected to occur, forming hydroxypropylene bridges between the diphenol subunits. These products are expected to be the most stable formed in an equilibrium of exchange reactions. Generally, in ether-exchange reactions, the formation of alcohols, phenols, aldehydes, and olefins are well-known degradation products for polyethers.⁹ These reactions may occur in the aliphatic regions of the resins investigated.

The degradation pathway is strongly influenced by the structure of the additional diamine subunits. Structural

effects must be taken into account as shown by the different results for the two samples containing diamine subunits. In general, for both samples the amines promote the formation of aldehyde end groups.

The thermal degradation of the polymer cured with MeHHPA differs greatly between Py-GC/MS and Py-FIMS. Only low amounts of MeHHPA as thermal degradation product are obtained with FIMS, whereas its formation is the main reaction under Py-GC/MS conditions. Hydrogen transfer from the hydroxypropylene group forming a carboxylic acid group can be expected, followed by condensation leading to MeHHPA. In contrast, hydrogen transfer from the MeHHPA subunit forming one ketene and one dihydroxypropyl end group is favored under the selected FIMS conditions.

As aryl-oxygen bonds are more stable than alkyl-oxygen bonds, the thermal degradation takes place in the aliphatic regions of the polymer, and the aryl-oxygen bonds remain intact. The thermal degradation of the samples based on TGETE starts with cleavage of the very weak aliphatic carbon-carbon bond of the tetraphenylethane subunits. Degradation reactions in the aliphatic region of the polymer follow, which are the same as observed for the polymers based on DGEBA.

Summarizing, it is clear that Py-FIMS is an efficient method for the investigation of epoxy resins and allows the identification of free volatiles as well as high-mass subunits in the polymer structure in a single measurement. It is noteworthy that the introduced method not only is capable for the well-known characterization of linear polymers but also serves as a powerful analytical tool for cross-linked polymers.

Acknowledgment. This work has been supported by the Deutsche Forschungsgemeinschaft, Bonn-Bad Godesberg (Schu 416/8-1). The gift of the polymer samples and constructive comments of Prof. S. Tsuge, Nagoya, Japan, are gratefully acknowledged. We thank Prof. K. H. König, University of Frankfurt, for his support and encouragement.

Registry No. DGEBA (homopolymer), 25085-99-8; (DGEBA)(DDM) (copolymer), 26376-58-9; (DGEBA)(*m*-xylenediamine) (copolymer), 110839-13-9; (DGEBA)(MeHHPA) (copolymer), 110233-19-7; TGETE (homopolymer), 30621-65-9; (TGETE)-(DDM) (copolymer), 110839-14-0.

References and Notes

- (1) Schulten, H.-R.; Lattimer, R. P. *Mass Spectrom. Rev.* **1984**, *3*, 231.
- (2) Foti, S.; Montaudo, G. In *Analysis of Polymer Systems*; Bark, L. S., Allen, N. S., Eds.; Applied Science: London, 1982; Chapter 5, p 109.
- (3) Schulten, H.-R.; Halket, J. M. *Org. Mass Spectrom.* **1986**, *21*, 613.
- (4) Schulten, H.-R. *J. Anal. Appl. Pyrolysis* **1984**, *6*, 251.
- (5) Schulten, H.-R.; Plage, B.; Ohtani, H.; Tsuge, S. *Angew. Makromol. Chem.* **1987**, *115*, 1.
- (6) Schulten, H.-R.; Plage, B. *J. Polym. Sci., Polym. Chem. Ed.*, in press.
- (7) Nakagawa, H.; Tsuge, S. *J. Anal. Appl. Pyrolysis* **1987**, *12*, 97.
- (8) Schulten, H.-R.; Simmleit, N.; Müller, R. *Anal. Chem.* **1987**, *59*, 2903.
- (9) Montaudo, G.; Puglisi, C. In *Developments in Polymer Degradation*; Grassie, N., Ed.; Applied Science: London, 1987; Vol. 7, Chapter 2, p 35.
- (10) Montaudo, G.; Puglisi, C.; Scamporrino, E.; Vitalini, D. *Macromolecules* **1986**, *19*, 870.
- (11) Grassie, N.; Guy, M. I. *Polym. Degrad. Stab.* **1985**, *13*, 11.
- (12) Lüderwald, I.; Urrutia, H. *Makromol. Chem.* **1976**, *177*, 2093.
- (13) Garozzo, D.; Giuffrida, M.; Montaudo, G. *Macromolecules* **1986**, *19*, 1643.
- (14) Schulten, H.-R.; Plage, B., unpublished results.